Materials Letters 137 (2014) 132–135

Contents lists available at ScienceDirect

Materials Letters

journal homepage: www.elsevier.com/locate/matlet

The influence of Ni layer and thickness of AZO layers on the optoelectronic properties of AZO/Ni/AZO tri-layer deposited at room temperature

M. Melvin David Kumar [a,b], Seon Mi Baek [b], Joondong Kim [a,b,*]

[a] Department of Electrical Engineering, Incheon National University, Incheon 406772, South Korea
[b] Photoelectric and Energy Device Application Lab (PEDAL), Incheon National University, Incheon 406772, South Korea

ARTICLE INFO

Article history:
Received 17 June 2014
Accepted 1 September 2014
Available online 6 September 2014

Keywords:
AZO film
Ni-insertion
AZO/Ni/AZO tri-layer
Carrier mobility
Optoelectronic properties

ABSTRACT

A thin Ni film was employed to improve electrical performances of aluminum-doped-zinc-oxide (AZO). AZO thickness was modulated to find an optimum combination for AZO/Ni/AZO tri-layer. A combination of AZO/Ni/AZO (50 nm/5 nm/50 nm) substantially improves carrier mobility 34.5 $cm^2 V^{-1} S^{-1}$ from 1.96 $cm^2 V^{-1} S^{-1}$ of bilayer AZO/AZO (50 nm/50 nm) film. Although, Ni-insertion sacrifices the optical transmittance, the AZO/Ni/AZO structure effectively enhances the figure of merit (FOM) values. We report that the optical and electrical properties of AZO layers could be enriched by embedding a thin Ni film in AZO layers with tuning the thickness of AZO layers.

1. Introduction

The contribution of transparent conductive oxide (TCO) layers in enhancing the properties of photoelectric devices such as solar cell, LED, photodiode etc., is peerless in the present decade [1–3]. Among TCO layers, indium-tin-oxide (ITO) layers were mostly used in photoelectric devices due to its excellent electrical properties. However, as ITO layers have a crucial limit for using expensive and rare indium material, ITO layers are gradually replaced by other oxide materials such as AZO [4], LaAlO3, SrTiO3[5], CdO [6] and SnO_2[7]. In the present work, metal embedded AZO layers were studied. The main drawback of AZO layers is to require a high processing temperature to achieve good electrical conductivity, which substantially limits TCO applications for flexible electronics [3].

High efficient photoelectric devices using AZO layers were reported by many researchers [8–11]. In order to increase the conductivity, thin metal layers such as Ni, Au, Ag, Al were embedded with AZO layers. Thin metal layers embedded in between two dielectric AZO layers can suppress the reflection from metal layer and thus achieving selective transparency in visible region [12]. The tri-layer devices of AZO/Au/AZO [13], AZO/Ag/AZO [14], AZO/Al/AZO [4] and AZO/Mo/AZO [15] combinations have been reported and all exhibited enhanced photoelectric performance. When compared to other metal layers, reflectivity of Ni is lower than that of Au and Ag, so that, increasing quantum efficiency which relates with absorption of photons [16].

As it is important to analyze the optical and electrical properties of AZO/Ni/AZO tri-layer combinations and so far, no studies were reported on AZO/Ni/AZO samples to the best of our knowledge, we prepared AZO/Ni/AZO tri-layer and AZO/AZO bilayer samples to study the influence of Ni in AZO layers and compare their properties with respect to layer thicknesses.

In this study, a thin layer of Ni was deposited in between two AZO layers to make AZO/Ni/AZO tri-layer combination. Each layer was deposited at room temperature. The structural, optical and electrical properties of AZO/Ni/AZO sample were compared with those of AZO/AZO bilayer film which is free of Ni layer. Then, the thickness of AZO layers was varied in the AZO/Ni/AZO tri-layer sample and characterized to find out the optimum thicknesses of AZO layers for AZO/Ni/AZO combinations. This study provides a design scheme for high-quality TCO film growth at a low thermal budget.

2. Experiment procedures

AZO/AZO bilayer film and AZO/Ni/AZO tri-layer film were prepared on Si and glass substrates by varying the layer thickness. Each layer was deposited by a sputtering system at room temperature. The AZO layer was deposited using RF magnetron sputtering method. We prepared a bilayer AZO film, which was deposited two-step AZO deposition of 50 nm each. Thereafter, this sample is referred as sample S1 (AZO/AZO = 50 nm/50 nm). In order to fabricate tri-layer samples, 5 nm thin Ni film was deposited by DC sputtering, followed

* Corresponding author at: Department of Electrical Engineering, Incheon National University, Incheon 406772, South Korea. Tel.: +82 32 835 8770; fax: +82 32 835 0773.
E-mail address: joonkim@incheon.ac.kr (J. Kim).

http://dx.doi.org/10.1016/j.matlet.2014.09.001
0167-577X/

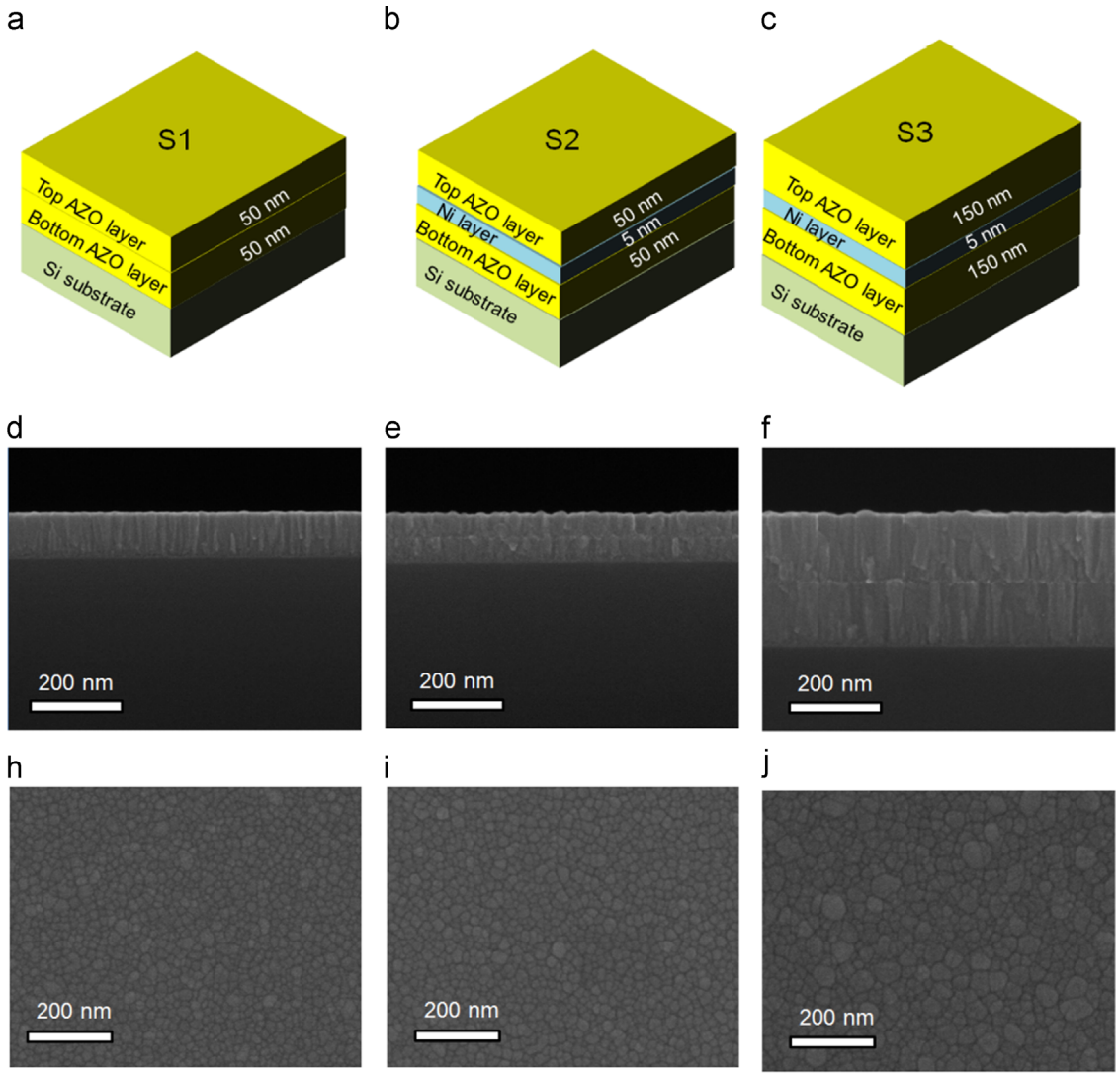

Fig. 1. Schematic diagram of samples (a) S1, (b) S2 and (c) S3. Cross-sectional and surface morphology FESEM images of (d, h) AZO/AZO (50/50 nm); (e, i) AZO/Ni/AZO (50/5/50 nm) and (f, j) AZO/Ni/AZO (150/5/150 nm) samples.

by a bottom AZO deposition. After then, a top AZO film was deposited on the Ni layer, to give AZO/Ni/AZO structure. We modulated the top and bottom AZO film thickness by 50 nm or 150 nm. Thereafter, we refer tri-layer sample S2 for AZO/Ni/AZO = 50 nm/5 nm/50 nm. Similarly, sample S3 for AZO/Ni/AZO = 150 nm/5 nm/150 nm. We prepared another sample of AZO/Ni/AZO with 250 nm/5 nm/250 nm thicknesses to find out the critical thickness for AZO layers. But, as this sample showed high resistivity of $1.63 \times 10^{-2}\ \Omega$ cm and low transmittance of 65.08%, these results were not included in the discussion.

Rapid thermal annealing was performed all samples for 10 min. The schematic diagram of samples S1, S2 and S3 are given in Fig. 1(a), (b) and (c), respectively. A field emission scanning electron microscope (FESEM, FEI Sirion) was used to observe the cross-sectional and top view images of prepared samples. The samples deposited on glass substrates were used to measure the optical properties of the samples with a UV spectrophotometer (Scinco, Neosys-2000).

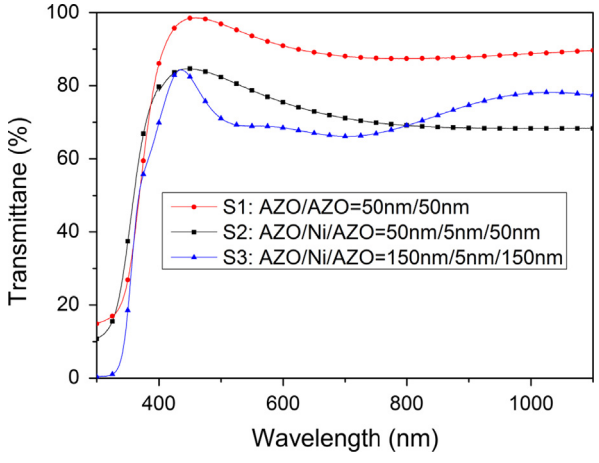

Fig. 2. Optical transmittance spectra of samples S1, S2 and S3.

3. Results and discussions

We prepared three different AZO samples, which are schematically presented in Fig. 1(a–c). Fig. 1(d–j) shows the cross-sectional and top view images of samples S1, S2 and S3. In the cross-sectional view of sample S1 (Fig. 1d), the continuous growth of 100 nm thick AZO layer was observed whereas, a thin Ni layer embedded between two AZO layers was seen in Fig. 1(e and f).

Since there was clear boundary between Ni and AZO layers, both top and bottom layers of AZO showed a similar dense and columnar

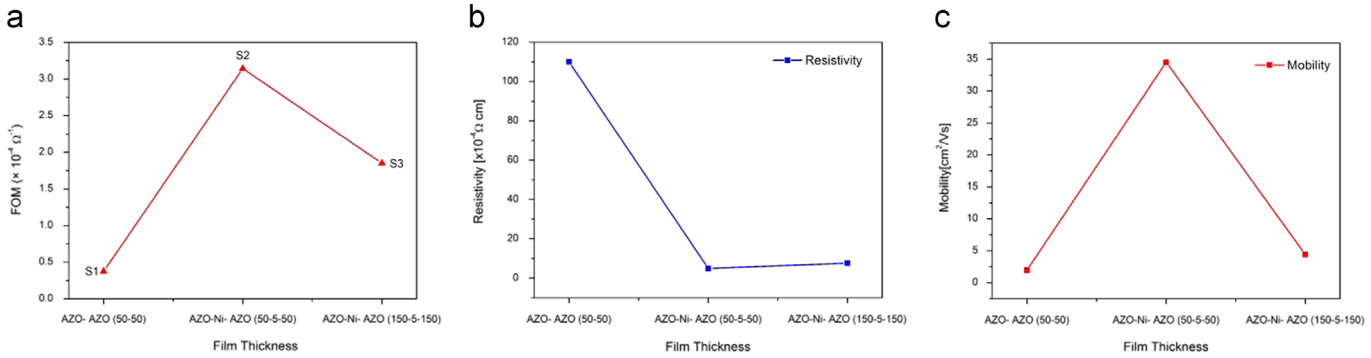

Fig. 3. (a) The figure of merit (FOM) for samples S1, S2 and S3 as a function of film thickness, (b) electrical resistivity and (c) Hall mobility of samples S1, S2 and S3 as a function of film thickness.

growth. In the top view of the prepared samples (Fig. 1h–j), uniform distribution of grains on the surface was observed. The grain size in sample S3 (Fig. 1j) was comparatively larger which indicates that the grain size increases with increasing thickness of AZO layers. The inhomogeneous grain structures in surface images arose due to the amorphous nature of AZO layers [15].

The thickness of metal layer plays an important role in determining optical transmittance and electrical conductivity of the device. Kim et al. [17] reported in their studies that the TCO sample exhibits low transmittance value of 27% when the thickness of intersecting Ni layer is increased to 20 nm. Ghosh et al. [18] has presented that Ni film of 5 nm thickness has the proficiency to reduce the resistivity of TCO layers without degrading much of its transmittance. Thus, 5 nm is the optimum thickness for Ni layer when it is deposited in between TCO layers [18].

Fig. 2 shows the optical transmittance of the samples S1, S2 and S3 as a function of wavelength. The highest transmittance of 98.52% was exhibited by single AZO layer of 100 nm thickness. Due to the higher conductivity and opaque nature of Ni layer, the average transmittance of the sample S2 has been reduced to 77.14%. Yu et al. [14] reported that when the thickness of AZO layers increases more than 100 nm, the average transmittance of the samples decreases. Hence, the transmittance value is further reduced to 70.38% in sample S3. At a wavelength of ~450 nm, maximum transmittance of 84.70% and 84.33% was exhibited by the samples S2 and S3, respectively. From the literatures, the maximum transmittance values of AZO/Au/AZO, AZO/Ag/AZO and AZO/Mo/AZO samples were found to be 83% [19], 62% [20] and 80% [15], respectively. In the present case, the sample S2 showed comparatively higher transmittance value. This is due to the presence of ultrathin Ni layer. Because of low reflectivity of Ni, more number of incident photons was transferred into AZO layers.

Resistivity (ρ) is directly proportional to sheet resistance (R_s) and total thickness (t) of the sample, i.e., $\rho = R_s \times t$ [21]. The sheet resistances of the prepared samples S1, S2 and S3 were calculated as 10940, 493.54 and 265.31 Ω/□, respectively. The AZO bilayer sample (S1) showed higher sheet resistance than that of samples S2 and S3. Haacke [22] proposed a method called figure of merit, FOM (ϕ_{TC}) which evaluates the overall performance of transparent conductors and it can be determined as

$$\phi_{TC} = \frac{T^{10}}{R_S} \quad (1)$$

where T is the transmittance at a wavelength of 480 nm and R_s is sheet resistance. The calculated FOM for samples S1, S2 and S3 were 0.375×10^{-4}, 3.14×10^{-4} and $1.85 \times 10^{-4}\ \Omega^{-1}$, respectively. The FOM of prepared samples as a function of layer thickness was given in Fig. 3(a). Since the noble metals offered less sheet resistance, the FOM value for AZO layers embedding with Au and Ag is a bit higher [19,20]. The maximum FOM value is found in sample S2. This indicates that AZO/Ni/AZO tri-layer with optimum layer thickness could offer enhanced optical and electrical properties in photoelectric devices.

Table 1
Optical and electrical properties of prepared samples.

	S1 (AZO/AZO)	S2 (AZO/Ni/AZO)	S3 (AZO/Ni/AZO)
Top AZO (nm)	50	50	150
Ni layer (nm)	0	5	5
Bottom AZO (nm)	50	50	150
Max. transmittance (%)	98.52	84.70	84.33
Mobility ($cm^2\ V^{-1}\ S^{-1}$)	1.96	34.5	4.41
Resistivity ($\times 10^{-3}\ \Omega$ cm)	110	4.86	7.54
Sheet resistance (Ω/□)	10940	493.54	265.31
FOM ($\times 10^{-4}\ \Omega^{-1}$)	0.375	3.14	1.85

The resistivity and mobility of prepared samples were shown in Fig. 3(b and c), respectively. Since Ni layer injects charge carriers into AZO layers, the resistivity of the Ni embedding samples is lower than that of ordinary AZO film. When the thickness of AZO layers increased from 50 to 150 nm, the mobility of sample S3 is dropped down from 34.5 to 4.41 cm^2/Vs. The mobility of sample S2 (34.5 cm^2/Vs) is higher than the reported values of 29.66 and 12.75 cm^2/Vs for AZO/Au/AZO [13] and AZO/Mo/AZO [15] samples, respectively. It is observed from Fig. 3 that the sample S2 showed better performance in both resistivity and conductivity. The electrical properties of prepared samples are given in Table 1.

Even though, the sample S1 offers high transmittance, its mobility is found to be too lower than the sample S2. In the same way, though the sample S3 showed low resistivity, there is no appreciative progress in mobility. The best fit of tri-layer combination (AZO/Ni/AZO) and layer thicknesses (50/5/50 nm) in sample S2 have made it to attain the transparency of 84.70% and the lower electrical resistivity of $4.86 \times 10^{-3}\ \Omega$ cm.

4. Conclusion

The structural, optical and electrical characteristics of bilayer AZO of 100 nm thickness, AZO/Ni/AZO tri-layer with thickness of 50/5/50 nm and AZO/Ni/AZO tri-layer with thickness of 150/5/150 nm samples were systematically analyzed. In this study, the influence of Ni layer and optimum thickness for top and bottom AZO layers in AZO/Ni/AZO tri-layer combination were reported. The embedded Ni layer is reduced the resistivity and enhanced the mobility of AZO/Ni/AZO sample. The 50 nm-thick AZO layers provided compromised transmittance without affecting mobility of charge carriers to AZO/Ni/AZO tri-layer combination. The FOM of sample S2 is found to be

higher ($3.14 \times 10^{-4}\,\Omega^{-1}$) than other two characterized samples S1 and S3. Therefore, it is concluded that the tri-layer sample AZO/Ni/AZO with the layer thickness of 50/5/50 nm promises for lower resistance, higher conductivity and improved transmittance for photoelectric applications.

Acknowledgments

The authors acknowledge the financial support of the Korea Institute of Energy Technology Evaluation and Planning, in a grant funded by the Ministry of Knowledge and Economy (KETEP-20133030011000).

References

[1] Lunt RR, Bulovic V. Appl Phys Lett 2011;98:113305.
[2] Young Margaret, Traverse Christopher J, Pandey Richa, Barr Miles C, Lunt Richard R. Appl Phys Lett 2013;103:133304.
[3] Kim Hyunki, Hong Seung-Hyouk, Park Yun Chang, Lee Jaekuen, Jeon Chil-Hwan, Kim Joondong. Mater Lett 2014;115:45–8.
[4] Lin Yen-sheng, Wei-Chihtseng. J Electron Mater 2012;41:438–41.
[5] Banerjee N, Huijben M, Koster G, Rijnders G. Appl Phys Lett 2012;100:041601.
[6] Zhu Y, Mendelsberg RJ, Zhu J, Han J, Anders A. Appl Surf Sci 2013;265:738–44.
[7] Wang Mi, Gao Y, Chen Z, Cao C, Zhou J, Dai L, et al. Thin Solid Films 2013;544:419–26.
[8] Khalid Mahmood, Hyun Wook Kang, Rahim Munir, Hyung Jin Sung. R Soc Chem Adv 2013;3:25136–44.
[9] Jiang QJ, Lun JG, Yuan YL, Cai H, Zhang J, Deng N, et al. Mater Lett 2014;123:14–8.
[10] Wang Chao, Mao Yanli, Zeng Xiangbo. Appl Phys A 2013;110:41–5.
[11] Boscarino S, Crupi I, Mirabella S, Simone F, Terrasi A. Appl Phys A 2014;116:1287–91. http://dx.doi.org/10.1007/s00339-014-8222-9.
[12] Sahu DR, Lin SY, Huang JL. Thin Solid Films 2008;516:4728–32.
[13] Chien-Hsun Chua, Hung-Wei Wub, Jow-Lay Huang. Mater Sci Eng B 2014;186:117–21.
[14] Jung Yu Sup, Park Yong Seo, Kim Kyung Hwan, Lee Won-Jae. Trans Electr Electron Mater 2013;14:9–11.
[15] Hung-Wei Wu, Chu Chien-Hsun. Mater Lett 2013;105:65–7.
[16] Giurgola S, Vergani P, Lucchi F, Pruneri V. Lasers and electro-optics.In: Proceedings of the international quantum electronics conference. CLEOE-IQEC 2007. European conference; 2007, (1) 17, (http://dx.doi.org/10.1109/CLEOE-IQEC.2007.4386181).
[17] Kim JC, Shin CH, Jeong CW, Kwon YJ, Park JH, Kim Daeil. Nucl Instrum Methods Phys Res B 2010;268:131.
[18] Ghosh DS, Martinez L, Giurgola S, Vergani P, Pruneri V. Opt Lett 2009;34:325.
[19] Tak YH, Kim KB, Park HG, Lee KH, Lee JR. Thin Solid Films 2002;411:12–6.
[20] Fahland M, Karlsson P, Charton C. Thin Solid Films 2001;392:334–7.
[21] Kloppel A, Kriegseis W, Meyer B, Scharmann A, Daube C, Stollenwerk J, et al. Thin Solid Films 2000;365:139–46.
[22] Haacke G. J Appl Phys 1976;47:4086.